WINDOWING OF WIDE-BAND ULTRASOUND TRANSDUCERS

Chris M.W. Daft and William E. Engeler

GE Corporate Research and Development
PO Box 8, Schenectady, NY 12301-0008
daft@crd.ge.com

ABSTRACT

A high performance ultrasound imaging system requires precise control of the amplitude of the elements in its aperture, as well as the time delays between them. We describe results in imaging with and without such apodizing, and describe a method for controlling channel amplitude which preserves the autonomy between channels characteristic of digital beamformers. As part of the study, we investigate how the classical results on windowing transfer to a high-bandwidth system such as an ultrasound scanner.

The algorithm allows the array to be dynamically windowed while its aperture grows in proportion to the time after a transmit excitation. Linear and curved arrays, where the phase center changes with beam position, are also accommodated. A surprisingly versatile system is needed to provide a satisfactory apodizing function in all cases. The simulations from a bit-level model of the VLSI implementation of the algorithm show its value in improving beam quality.

1. INTRODUCTION

The question of how best to window an imaging aperture is an old one, and the subject of numerous articles, since it overlaps with more general topics in spectral estimation [1] and harmonic analysis [2]. It has also been termed "shading", "blooming" or "apodizing", depending on the particular area of imaging theory under discussion. Wright [3] and Maslak [4] emphasized the importance of windowing in commercial phased-array instruments more than a decade ago. Their contention was that *detail resolution*—determined by beamformer accuracy, transducer width and frequency—is inadequate to measure the performance of an imager. This is because the clinician is also concerned with differentiating between small changes in texture and contrast. As an example, most older people have cysts (fluid-filled spheres) resulting from injuries; these structures are benign. Often, tumors are almost as hypoechoic as cysts, but require immediate attention. The amount of energy emitted by the transducer away from the main beam direction is thus of great interest; the term *contrast resolution* has been coined as a measure of it.

This paper examines windowing, or apodizing, the array in view of various complications inherent in the ultrasonic case. It presents a method for achieving accurate channel-based amplitude control, and shows results from simulations of an imager.

2. ULTRASOUND APODIZING *VS.* SPECTRAL WINDOWING

The ultrasound imaging problem can broadly be understood in terms of Fourier optics, an appealing framework with which to create intuition about imaging performance A basic imaging equation [6] can be formed from the integral of the Green's function multiplied by the aperture function, both expanded to quadratic terms:

$$\phi(r,\theta) \propto \frac{e^{ikr}}{r}\int_{x_l}^{x_r} e^{ik[x\sin\theta+x^2\cos^2\theta/2r]}\cdot e^{-ik[x\sin\theta_0+x^2\cos^2\theta_0/2r_0]}W(x)dx. \quad (1)$$

In equation (1), ϕ is the velocity potential at (r,θ); the focus of the imager is at (r_0,θ_0); the wavenumber $k=2\pi/\lambda$; and $W(x)$ is the window function of the aperture, which extends from x_l to x_r. This is a far-field, narrowband approximation, and looks like a Fourier transform in the variable $kx(\sin\theta-\sin\theta_0)$ close to the focal point of a near-field imager such as an ultrasound machine. In this regime, for a continuous-wave excitation, the beam bears a Fourier transform relation to aperture amplitude. Therefore, by employing a windowing scheme [2], we would expect to decrease the unwanted energy in the imager's sibelobes, at the cost of a loss of detail resolution. Two features of ultrasound transducers make this a more complex scenario, however. These are the wide fractional bandwidths used in ultrasound, and the directivity of the individual transducer elements.

2.1. Effect of wide bandwidth

Equation (1) gives the field for continuous-wave excitation. In recent years, typical commercial transducers have expanded their -3 dB fractional bandwidths from 40% to around 70%, so it is necessary to understand the effect on the point-spread function of "white light" illumination of the aperture. (Fractional bandwidths will be quoted as full-widths at the half-power point of the spectrum). Nikoonahad [5] derived an equation for the point-spread function of a circular aperture excited with a toneburst pulse of length T, with no windowing:

$$B(R)=\int_{-\infty}^{\infty}\left[\frac{J_1(\pi R)}{\pi R}\right]^2 \mathrm{sinc}[T(f-f_0)]df, \quad (2)$$

where f_0 is the center frequency of the toneburst, D is the aperture diameter, and $R=kDr/2\pi r_0$. The squared Bessel

0-7803-3615-1/96/$5.00

function term results from this equation describing a two-way beam, in contrast to (1). The effect of broadband transducer excitation is thus twofold:

- As the frequency increases, the focus becomes tighter.
- The point-spread function at a given frequency is added to the integral with a "weight" given by the amplitude of the Fourier transform of the excitation at that frequency.

While this allows us to predict resolution of a broadband system based on the *center of gravity* (or first moment) of the power spectrum, the effect of a window is less clear. As a first step in understanding this, we simulated a 64λ sector probe at low (8%) and high (70%) bandwidths, with and without shading. The excitation was a Gaussian-modulated sine wave (center frequency 3.75 MHz), and a Tukey window function was used. The simulation was designed to accurately reflect the operating constraints of a real-life imager. Round-off and quantization noise (in both amplitude and time-delay) thus limit the effects of the windowing.

In the narrowband (figure 1) and wideband (figure 2) plots, the windowed array is represented by the solid line; the unshaded array is dotted. The beam profiles plotted are maximum intensity projections of the point-spread function. Zero degrees on the abscissa refers to the direction broadside to the array. The simulated point source is positioned 7.2° off-axis, at a range of 50 mm.

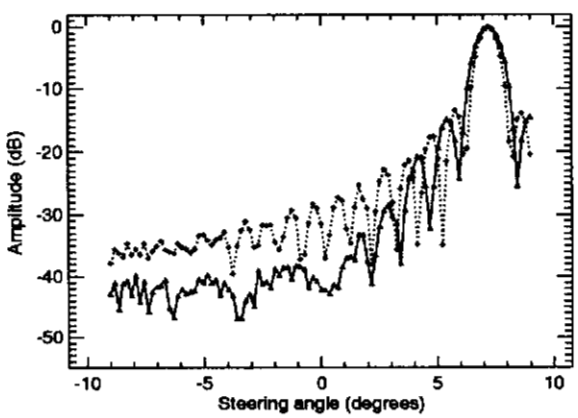

Figure 1: Effect of windowing with 8% fractional bandwidth. The windowed array is the solid line; the unshaded array is dotted. The windowing trades off main lobe width and sidelobe level.

A moderate improvement in the sidelobe energy is evident in both the narrow-band and wideband cases. For many transducers, however, windowing is more necessary than these examples suggest.

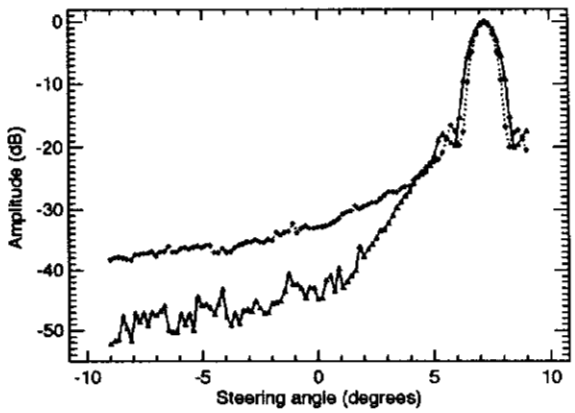

Figure 2: Effect of windowing with 70% fractional bandwidth. The windowed array is the solid line; the unshaded array is dotted. The "white-light" effect is apparent, in that oscillations in the beam profile have disappeared; however, windowing still proves useful.

2.2. Element directivity

An approximation for the directivity of a transducer element of width Δx is given by

$$D(\alpha) = \cos(\alpha)\mathrm{sinc}\left[\frac{k\Delta x}{2}\sin\alpha\right]. \qquad (3)$$

The cosine term is a consequence of the high-impedance PZT operating into relatively low-impedance tissue; the sinc term is the diffraction pattern of a line receiver of sound. This directivity depends on the angle α between the transducer element and the source of sound, and it is superimposed upon any windowing in a manner dependent upon the source location. The significance of this equation can be seen by evaluating it for sector and linear trasnducers operated at $F/2$. For a $\lambda/2$ sector probe, D varies from 1 to 0.82 for the $\theta = 0$ beam; thus the elements appear largely point-like and omnidirectional. However, with a $3\lambda/2$ linear transducer, the variation in D is from 1 to 0.36. This means that the coherent sum from such an array, receiving from a point source at x_b,

$$\text{beamsum} \propto \int_{x_l}^{x_r} D[\alpha(x - x_b)]dx, \qquad (4)$$

is considerably smaller than the $(x_r - x_l)/\Delta x$ one might expect without directivity effects.

The sidelobe level is determined by a similar integral, which includes a sinusoidal term indicating the angle of steering error; for a beam focused at x_b, the signal received from a source at x_s is

$$\text{sidelobe} \propto \int_{x_l}^{x_r} D[\alpha(x - x_s)]e^{i\xi(x_b,x_s)x}dx. \qquad (5)$$

The factor $e^{i\xi(x_b,x_s)x}$, which induces a phase shift across the array, means that essentially only the values of D at

the ends of the integral contribute to the sidelobe level in the unwindowed case. If we are unlucky enough to have the interfering source position x_s at either end of the currently active aperture ($x_s = x_l$ or $x_s = x_r$), $D = 1$ and the end effect is magnified with respect to the coherent sum. Therefore, care should be taken with directive linear transducer elements, since their sidelobes are more serious. This is illustrated in figure 3, where the difference between the windowed and unwindowed beam profiles is very significant.

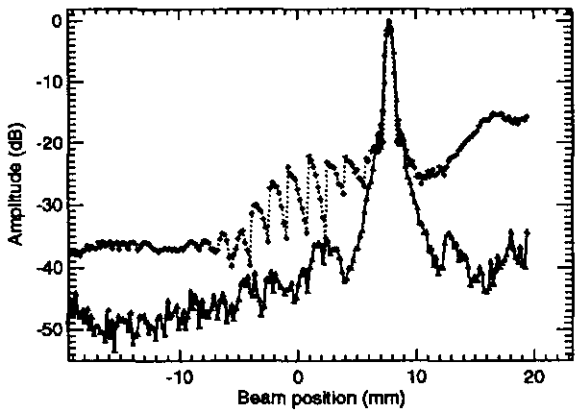

Figure 3: Effect of windowing on a 7.5 MHz linear array with λ element spacing. The fact that the end elements in the windowed array are always operated at a low amplitude reduces the problem of "sidelobe amplification" characteristic of large linear probe elements. The oscillating behavior seen in the unwindowed (dotted) line is characteristic of changes in the array multiplexing. This reinforces the idea that we are dealing with an end effect.

3. IMPLEMENTATION

A premium imager needs to adjust both time delay and amplitude continuously, for each receive channel. This is because the "dynamic focus" requires a lens whose strength decreases with range. The aperture increases with range, so we need to dilate and translate the tapering function to reflect the dynamics of the aperture. We would like to generate a function of time t for each channel of the imager $W(x,t)$

$$W(x,t) = f\left[\frac{x + c(t)}{w(t)}\right], \tag{6}$$

which looks like figure 4. In this diagram, the straight lines show a constant F-number. The physical dimensions of the array limit the growth of the aperture at n_e and n_m. This also explains why translation as well as dilation of the window is necessary.

In (6), W is the window function, $w(t)$ is its width, and $c(t)$ is its offset from the center of the aperture. Dynamic windowing is complicated for linear and curvilinear transducers, because the phase center and the physical center of

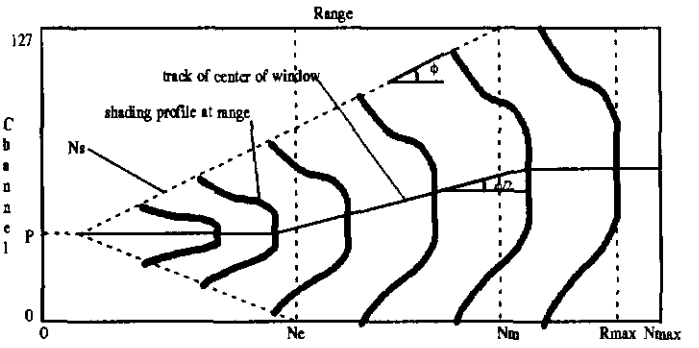

Figure 4: Approximate form of $W(x,t)$ for linear array where beam position is offset from array center. Note the need to translate the center of the window function (as well as dilating it) as the range increases and the aperture enlarges. This is due to the effect of the physical extremities of the transducer.

the aperture aren't coincident. The functional dependence f is easily implemented using a RAM; the rest of the circuit makes the address of that RAM. The fundamental problem is that while $c(t)$ and $w(t)$ have simple functional forms when viewed from the perspective of the entire aperture:

$$w(t) = k_1 t \tag{7}$$

$$c(t) = \begin{cases} p & \text{if } n \le n_e \\ p + k_2 t & n_e < n \le n_m \\ x\text{max}/2 & n > n_m, \end{cases} \tag{8}$$

the dynamic windowing sees only the development of one channel's amplitude as a function of time. ($x_{\max}$ is half the extent of the aperture; p is its phase center; n is the clock count, and k_1 and k_2 are constants.) A good approximation to the rather awkward single-channel form treats the amplitude as a piecewise hyperbolic function:

$$y(n) = \begin{cases} 0 & \text{if } n < n_s \\ g_s n_s - g_s n_s^2/n & n_s < n \le n_e \\ g_e n_e + g_e n_e^2/n & n_e < n \le n_m \\ g_m n_m - g_m n_m^2/n & n > n_m. \end{cases} \tag{9}$$

This describes the most complex form of the address $y(n)$, which occurs when the parameters specifying the position of the channel in the aperture, n_s, n_e and n_m, are related by $n_s \le n_e \le n_m$. While we need to be able to produce up to three hyperbolas, and their signs may differ from those in equation (9), the function $y(n)$ can be assumed to be continuous. This is because the purpose of the dynamic windowing is to avoid any discontinuity in amplitude at any time during the opening of the aperture. A convenient algorithm to make such hyperbolic functions in VLSI [7] is Bresenham's algorithm [8]. An example of this type of algorithm (which was originally developed to efficiently draw curves on raster displays) is shown in figure 5.

```
a = ScaleParameter;
b = StartClock;
c = StartClock;
RamAddress = MemorySize;

for (n = StartClock; n < EndClock; n ++) {
   b ++;
   c -= a;
   if (c < 0) {
      a --;
      c += b;
      RamAddress --;
   }
}
```

Figure 5: Bresenham's algorithm, shown in a form which computes a hyperbola of a clock variable, n. This computation translates well into the types of operation possible at high speed within an ASIC.

The algorithm of figure 5 computes the function,

$$\text{RamAddress} = \text{ScaleParameter}\left[\frac{\text{StartClock}}{n} - 1\right], \quad (10)$$

which, with appropriate resets at n_e and n_m, can produce $W(x,t)$. It involves no divisions or nmultiplications. The output `RamAddress` can be connected to the address lines of a RAM containing an arbitrary window function f.

4. CONCLUSIONS

Windowing is an important topic for producing consistently artefact-free ultrasound images. The need is pronounced for transducers whose elements are appreciably larger than $\lambda/2$, which is often the case. Making a circuit which computes an adequate approximation to the desired window function is quite challenging, but worthwhile in terms of image quality.

There is obviously much more to investigate in this area. Further work might include calculating optimal windowing functions for transducers of varying bandwidth and element directivity. A measured impulse response should also replace the exponentially modulated sine wave used in these simulations; equation (2) shows that this will affect the results. The *effective aperture* [9] model of transmit-receive imaging demonstrates that this two-way process results in a self-convolution of the aperture window function. Then, for example, a square aperture amplitude becomes a triangular shape. In this case, there is a significant amount of self-windowing occuring. Perhaps when this is taken into account, the case for windowing the aperture will be less clear.

5. ACKNOWLEDGEMENTS

The authors would like to thank Wayne Rigby, Lewis (Tom) Thomas and Matt O'Donnell for many intriguing discussions of imaging, and Bill Leue (who composed figure 4), Carl Chalek, Bob Dunki-Jacobs and Bill Hatfield for enthusiastic software support of this work. Scott Smith originally motivated the investigation of array performance through simulation at CRD. The vision and execution of Sharbel Noujaim, John Pedicone and Ted Rhyne is much appreciated.

6. REFERENCES

[1] S.L. Marple, "Digital spectral analysis: with applications", Englewood Cliffs, NJ: Prentice-Hall, 1987.

[2] F.J. Harris, "On the Use of Windows for Harmonic Analysis with the Discrete Fourier Transform", *Proc. IEEE* **66**(1), 51–83 (1978).

[3] J.N. Wright, "Resolution issues in medical ultrasound", *Proc. IEEE 1985 Ultrasonics Symposium*, 793–799.

[4] S.H. Maslak, "Computed Sonography", in *Ultrasound Annual 1985*, ed. R.C. Saunders and M.C. Hill, New York: Raven Press.

[5] M. Nikoonahad and E.A. Ash, "Resolution of scanning ultrasonic imaging systems with arbitrary transducer excitation", *Revue Phys. Appl.* **20**, 383–389 (1985).

[6] G.S. Kino, "Acoustic waves: Devices, imaging and analog signal processing", 158–163. Englewood Cliffs, NJ: Prentice-Hall 1987.

[7] W.E. Engeler, C.M.W. Daft, J.T. Pedicone and T.L. Rhyne, "Ultrasound Imaging System with Dynamic Window Function", US Patent 5,345,939 (1994).

[8] J.E. Bresenham, "Algorithms for circular arc generation", in *Proc. NATO Advanced Study Institute*, 197–217, ed. R.A. Earnshaw. Berlin: Springer-Verlag 1986.

[9] R.Y. Chiao and L.J. Thomas, "Aperture Formation on Reduced-Channel Arrays Using the Transmit-Receive Apodization Matrix", *Proc. IEEE 1996 Ultrasonics Symposium.*